POLITECNICO DI TORINO
Repository ISTITUZIONALE

Comparison of Probabilistically Shaped 64QAM with Lower-Cardinality Uniform Constellations in Long-Haul Optical Systems

Original
Comparison of Probabilistically Shaped 64QAM with Lower-Cardinality Uniform Constellations in Long-Haul Optical Systems / Pilori, D., Bertignono, L., Nespola, A., Forghieri, F., Bosco, G.. - In: JOURNAL OF LIGHTWAVE TECHNOLOGY. - ISSN 0733-8724. - ELETTRONICO. - 36:2(2018), pp. 501-509. [10.1109/JLT.2017.2752842]

Availability:
This version is available at: 11583/2700118 since: 2018-03-06T09:05:36Z

Publisher:
Institute of Electrical and Electronics Engineers Inc.

Published
DOI:10.1109/JLT.2017.2752842

Terms of use:

This article is made available under terms and conditions as specified in the corresponding bibliographic description in the repository

Publisher copyright
IEEE postprint/Author's Accepted Manuscript

©2018 IEEE. Personal use of this material is permitted. Permission from IEEE must be obtained for all other uses, in any current or future media, including reprinting/republishing this material for advertising or promotional purposes, creating new collecting works, for resale or lists, or reuse of any copyrighted component of this work in other works.

(Article begins on next page)

26 November 2026

Check for updates

Macromolecular Rapid Communications

Macromolecular Rapid Communications
www.mrc-journal.de

RESEARCH ARTICLE OPEN ACCESS

Building From the Ground Up: A Procedural Guide to Locally Controlling Bond Exchange Kinetics in Dynamic Thiol-Thioester Networks

Roman Korotkov[1,4] | John Vincent Tumaneng[2] | Roberta Bongiovanni[2] | Sara Dalle Vacche[2] | Elisabeth Rossegger[1,3] | Sandra Schlögl[1,4]

[1]Polymer Competence Center Leoben GmbH, Leoben, Austria | [2]Department of Applied Science and Technology, Politecnico Di Torino, Turin, Italy | [3]Institute For Chemistry and Technology of Materials, Graz University of Technology, Graz, Austria | [4]Institute of Chemistry of Polymeric Materials, Technical University of Leoben, Leoben, Austria

Correspondence: Sara Dalle Vacche (sara.dallevacche@polito.it) | Elisabeth Rossegger (elisabeth.rossegger@pccl.at; elisabeth.rossegger@tugraz.at) | Sandra Schlögl (sandra.schloegl@pccl.at)

Received: 12 August 2025 | **Revised:** 1 September 2025 | **Accepted:** 9 September 2025

Funding: This project has received funding from the EU's Horizon 2021 programme under the Marie Skłodowska-Curie Doctoral Networks (MSCA-DN) grant agreement No 101073432. Part of the research work was also carried out within the COMET-Module project "Repairtecture" (project-no.: 904927) at the Polymer Competence Center Leoben GmbH (PCCL, Austria) within the framework of the COMET-program of the Federal Ministry for Climate Action, Environment, Energy, Mobility, Innovation and Technology and the Federal Ministry of Labor and Economy. Funding was received by the Austrian Government and the State Governments of Styria and Upper Austria.

Keywords: covalent adaptable networks | local deactivation | photoacid generator | photoswitchable polymer | thiol-thioester exchange

ABSTRACT

Covalent adaptable networks (CANs) are a new class of polymers possessing the structural robustness of classical thermosets and stimuli-dependent malleability of thermoplastics, imparting them with repairability, reprocessability, and recyclability potential. These CANs can even be tailored to have spatially controllable properties and enhanced functionality; however, the introduction of additional reactive moieties leads to inadvertent side reactions and deterioration of the desired performance. Herein, we present a comprehensive approach to the optimization of locally controllable CANs, relying on base catalyzed thiol-thioester exchange reactions. The network is formed by visible light (405/450 nm) induced radical thiol-ene polymerization, whilst local deactivation of the dynamic exchange reaction is achieved by neutralizing the basic catalyst with a photoacid generated upon UV-light (365 nm) exposure. The intricate interactions between the resin components were studied, and the factors affecting the network performance were investigated to provide a detailed account of the development process, from the rational selection of initial components to the systematic optimization of a locally controlled, photoswitchable CAN. Finally, its on-demand tunability is demonstrated by surface- and bulk shape reconfiguration through heat-assisted processes.

1 | Introduction

Covalent adaptable networks (CANs) are a class of polymers that find their place between classical thermosets and thermoplastic materials [1–8]. Without the application of an external stimulus, such materials behave like traditional covalently crosslinked polymer networks, which possess high thermal stability, chemical resistance, and high mechanical properties. Once a certain stimulus is applied, dynamic exchange reactions take place, resulting in the topological rearrangement of the polymeric network.

This is an open access article under the terms of the Creative Commons Attribution-NonCommercial License, which permits use, distribution and reproduction in any medium, provided the original work is properly cited and is not used for commercial purposes.
© 2025 The Author(s). *Macromolecular Rapid Communications* published by Wiley-VCH GmbH

This unique property allows CANs to be malleable, reshapeable, healable, and recyclable, similar to thermoplastics [7–11]. The majority of CANs rely on a thermal stimulus, but light, chemical agents, or ultrasound are also known to be used to activate the exchange reactions [8, 12–14]. Based on the mechanism of dynamic exchange reactions, CANs are divided into two subgroups: dissociative and associative. In case of dissociative CANs, the topological rearrangement proceeds through the breakage of a chemical bond at one place with further establishing of a new bond, which leads to a temporary decrease of the crosslink density of the network. In associative CANs, the exchange reactions happen through a transition state where the new covalent bond forms before the old one breaks. Thus, the structural integrity of the polymer is retained while undergoing a topology rearrangement [11, 15–17].

Leibler and co-authors introduced the term vitrimer for this type of CANs from their investigation of dynamic epoxy-acid and epoxy-anhydride networks, which underwent thermoactivated transesterification reactions [18]. Over the past years, various chemical mechanisms have been investigated for the design of associative CANs [19]. One rapid exchange reaction exploited in associative CANs is the thiol-thioester exchange reaction, which allows stress-relaxation to occur even at room temperature [20–22]. The transthioesterification is accelerated by basic catalysis, which opens the possibility to control the rate of exchange processes via selection of a suitable catalyst and by tuning the network [20, 23, 24].

However, most of the dynamic chemistries rely on thermoactivated dynamic reactions, which lack spatial control [25, 26]. CANs utilizing the thiol-thioester exchange reactions are no exception. Achieving spatial control for such dynamic networks is possible by the use of light-stimulated processes, such as the photo-thermal effect [27, 28] or the use of photosensitive compounds to locally tune the dynamics of topological rearrangement via shifting the concentration of the reactive groups, which participate in the exchange reactions [29, 30] or by light-induced release of the catalyst [31, 32]. The use of various photolatent bases and acids was deeply investigated in our group for the local control of bond exchange reactions in thermally and photochemically curable polymeric networks [21, 25, 26, 30].

In particular, the concept of chemical amplification upon the activation of a photoacid generator (PAG) with subsequent release of the hydroxyl groups was investigated for local control of transesterification kinetics [29, 30]. Besides that, in our previous work, we demonstrated an approach for further improvement of the activation resolution by introducing a covalently attachable photolatent catalyst (PAG-Vi) [26].

Along with the local activation of the dynamic exchange reaction via release of the catalyst, the spatially controlled deactivation of the exchange dynamics was shown by the Bowman group through the release of a catalyst scavenger in the system [22]. A deactivation of the exchange reactions is of particular interest for soft (with a glass transition temperature below room temperature) dynamic networks to avoid undesired creep during usage (e.g., once the material has been reshaped or reprocessed).

Inspired by this study, herein, we investigate the local deactivation of thiol-thioester exchange reactions through photolysis of a covalently attachable PAG in a photocurable thiol-ene photopolymer. The polymeric network was cured with 405 nm visible light (VIS-cured), and the local deactivation of the network's exchange dynamics was achieved by irradiation with 365 nm UV light (UV-deactivated), allowing patterning of the surface of the material by thermal imprinting. While previous studies have demonstrated spatial deactivation of dynamic chemistries in CANs, we highlight the effect of the interaction between resin components on the dynamic exchange kinetics. The orthogonality of the photoprocesses and intercomponent behavior was taken into careful consideration to establish a robust strategy in local control of dynamic exchange reactions and optimization of the photoswitchable dynamic photopolymer within a single thiol-thioester CAN. The established procedural framework identifies the critical parameters governing resin formulation and performance. By detailing the process from initial component selection down to the system optimization, we describe not only the creation of effective thiol-thioester CANs but also their refinement based on experimental outcomes. The intricate chemical interplay between photoinitiators, catalysts, and crosslinking agents requires careful navigation, which is a challenge we address through our targeted recommendations. Our goal is to establish a reliable methodology that researchers can adapt to their specific requirements, ultimately advancing the development of photoswitchable materials with precisely, locally controlled, and experimentally validated behavior.

2 | Results and Discussion

2.1 | Designing a Wavelength-Orthogonal System

The development of a thiol-thioester photoswitchable dynamic polymer requires careful consideration of material components and their specific interactions. Figure 1 lays out the components making the resin, while Table 1 lists the tested compositions and their respective labels. Thiol-ene photopolymers were selected as the matrix material due to their significant advantages in polymer synthesis. Their step-growth polymerization generally results in lower shrinkage and higher monomer conversion compared to traditional radical homopolymerization [23]. A critical aspect of this material's design involves the phototriggered processes of curing and deactivation. Curing relies on interactions between monomers to form the network, while the deactivation mechanism utilizes acid-base interactions to modulate the catalyst's activity and to control bond exchange dynamics. Moreover, a polymer's performance extends beyond a simple summation of individual component properties. Intricate chemical interactions necessitate precise balancing of components; as such, the initial research approach involves establishing a preliminary composition with strategically assigned component quantities.

The studied photopolymers were obtained using TEDAE monomer and PETMP crosslinker, keeping the ratio between –ene and thiol moieties equal to 1:2 to ensure an excess of free thiol functionalities that could facilitate thiol-thioester bond exchange reactions in the presence of TMG as basic catalyst. TPO-L was added as a long-wavelength-absorbing radical photoinitiator enabling network formation upon visible

15213927, 2025, 22, Downloaded from https://onlinelibrary.wiley.com/doi/10.1002/marc.202500654 by Politecnico Di Torino Sist. Bibl Del Polit Di Torino, Wiley Online Library on [10/12/2025]. See the Terms and Conditions (https://onlinelibrary.wiley.com/terms-and-conditions) on Wiley Online Library for rules of use; OA articles are governed by the applicable Creative Commons License

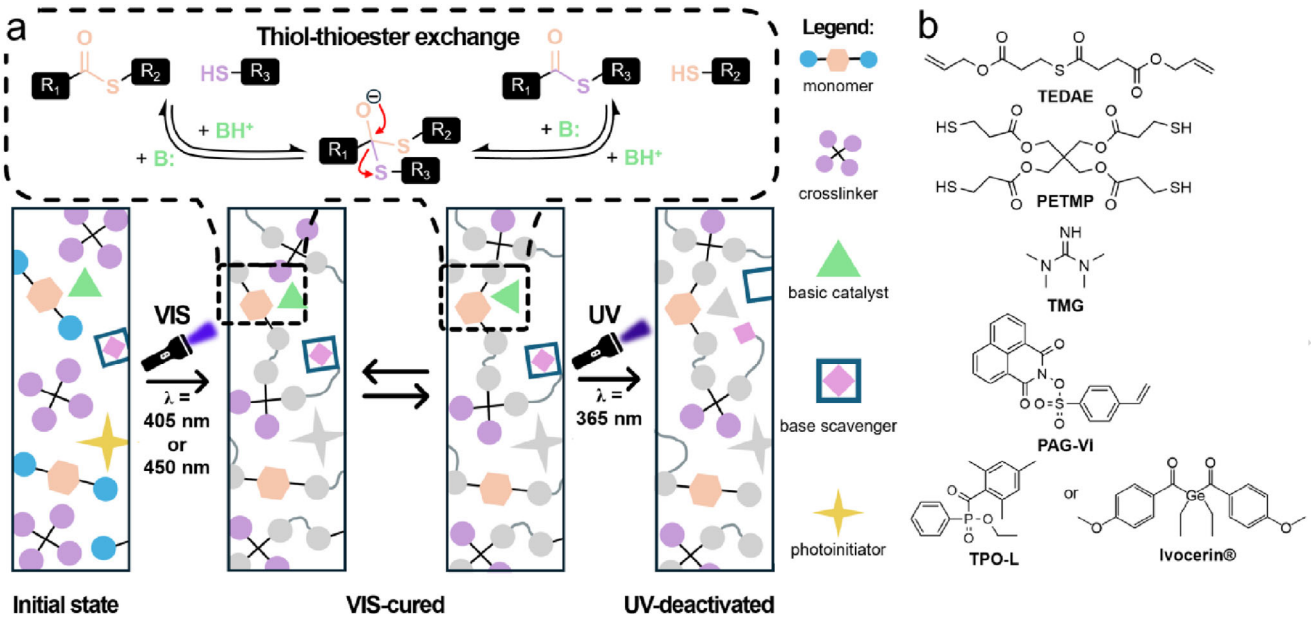

FIGURE 1 | (a) Illustration of the photoswitchable dynamic resin's components, photocuring, base-catalyzed thiol-thioester exchange, and deactivation by UV-induced release of an acid. (b) Chemical structures of the primary resin components.

TABLE 1 | Compositions (in mole equivalence) of studied formulations.

Sample name	TEDAE	PETMP	TPO-L	Ivocerin	TMG	DABCO	DBN	PAG-Vi
P0T0L2	1.00	1.00	0.02	—	—	—	—	—
P3T3L1	1.00	1.015	0.01	—	0.03	—	—	0.03
P3T3L2			0.02					
P3T3L5			0.05					
P0T3L1	1.00	1.00	0.01	—	0.03	—	—	—
P0T3L2			0.02					
P0T3L5			0.05					
P1T3L2	1.00	1.005	0.02	—	0.03	—	—	0.01
P2T3L2		1.010						0.02
P3T3L2		1.015						0.03
P0DABCO3L2	1.00	1.00	0.02	—	—	0.03	—	—
P3DABCO3L2		1.015						0.03
P0DBN3L2	1.00	1.00	0.02	—	—	—	0.03	—
P3DBN3L2		1.015						0.03
P3T3IVO1	1.00	1.015	—	0.01	0.03	—	—	0.03
P3T3IVO2				0.02				
P3T3IVO5				0.05				
P0T3IVO2	1.00	1.00	—	0.02	0.03	—	—	—

light exposure (405 nm). For the controlled deactivation of TMG in the photopolymer, a photoacid generator (PAG) with a non-overlapping absorption wavelength was chosen to avoid its premature release during the visible-light induced curing step. From the wide range of reported PAGs, PAG-Vi was selected due to its (1) absorption characteristics, (2) good solubility in PETMP, (3) non-ionic nature of the photo-cleavable group, and (4) ability to be immobilized within the network through its vinyl group that enables enhanced spatial control of the system. PAG-Vi is comprised of a photocleavable naphthalimide group covalently linked to a vinyl-functionalized aromatic sulfonic acid, which has a λ_{max} at 333 nm and is transparent in the visible light region. Absorption spectra of the radical photoinitiators and PAG-Vi are shown in Figure S1.

15213927, 2025, 22, Downloaded from https://onlinelibrary.wiley.com/doi/10.1002/marc.202500654 by Politecnico Di Torino Sist. Bibl Del Polit Di Torino, Wiley Online Library on [10/12/2025]. See the Terms and Conditions (https://onlinelibrary.wiley.com/terms-and-conditions) on Wiley Online Library for rules of use; OA articles are governed by the applicable Creative Commons License

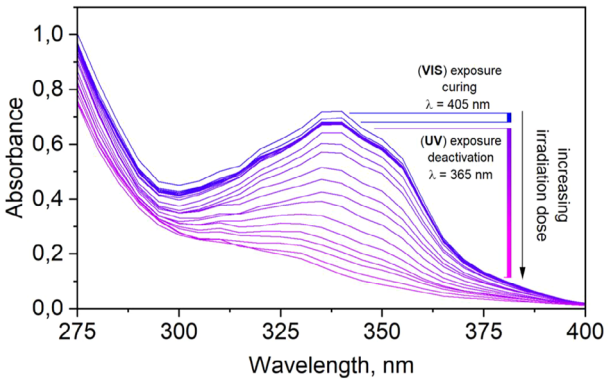

FIGURE 2 | UV–vis spectra of formulation containing 3 mol% of PAG-Vi, 3 mol% of TMG, and 2 mol% of TPO-L (P3T3L2) upon irradiation of 405 and 365 nm light as a function of the exposure dose.

However, despite the use of two different wavelengths for curing and activation of the PAG-Vi, claiming full orthogonality of the photocleavage reactions of TPO-L and PAG-Vi warrants further investigation. Our previous study, related to the use of the latter in photocurable thiol-ene vitrimers relying on a latent transesterification acidic catalyst, revealed that the photocleavage reactions of TPO-L and PAG-Vi are not fully orthogonal in thiol-ene photopolymers and that PAG-Vi is already activated during irradiation at 405 nm, albeit at a low extent (12%) [26]. This is also observed in the thiol-thioester resins under investigation containing TMG as a base catalyst. Figure 2 shows the UV–vis spectra of the thioester-thiol system with 3 mol% of PAG-Vi, 3 mol% of TMG and 2 mol% of TPO-L (P3T3L2). The broad absorption band (λ_{max} = 335 nm) can be related to PAG-Vi; however, TPO-L also possesses certain absorption, although relatively low, in this region. Upon photocuring at 405 nm this absorption band slightly decreases (5.6%), which could be associated with the photolysis of TPO-L as well as premature photocleavage of naphthalimide group of PAG-Vi. In contrast, subsequent UV irradiation (365 nm) leads to a fast and distinctive decrease of the absorption profile, giving rise to the efficient cleavage of the chromophore.

To improve the orthogonality between curing and acid release, two different strategies were pursued. On the one hand, the photoinitiator concentration was increased, and on the other hand, TPO-L was replaced by Ivocerin, which has an extended absorption profile in the visible light region and can be activated at 450 nm. At a higher TPO-L concentration (5 mol%), no clear decrease in the PAG-Vi absorption profile could be detected during curing (405 nm), which indicates an improved orthogonality due to an internal filter effect of the radical photoinitiator. In the case of the use of Ivocerin, the absorption spectra of PAG-Vi and the photoinitiator are strongly overlapping, and no clear conclusion could be made.

The influence of resin formulation on cure kinetics was examined in a stepwise manner using FTIR spectroscopy to monitor alkene and thiol conversion (Figure S2).

First, the influence of the basic catalyst on the curing of thiol-ene photopolymer was investigated with the use of TPO-L as photoinitiator on a base-free formulation (P0T0L2) and one containing TMG (P0T3L2). In the absence of TMG, efficient curing was observed, with rapid and high conversion of both alkene and thiol functional groups. The addition of TMG significantly reduced the cure rate. After exposure to a 405 nm lamp delivering a dose of 720 mJ·cm^{-2}, the maximum alkene conversion dropped from 99.90% for P0T0L2 (without TMG) to 91.37% for P0T3L2 (with TMG). This is attributed to the basic nature of TMG, which promotes the formation of thiolate species. These thiolates can react with free thiyl radicals to generate metastable disulfide radical anions that do not participate in chain propagation; thereby acting as inhibitors in the radical-mediated thiol–ene reaction. As a consequence, TMG not only acts as a basic catalyst but also introduces a decelerating effect on the curing kinetics due to radical scavenging behavior [33].

Second, the type and concentration of the photoinitiator also affect the cure kinetics. Under identical irradiation intensity (9.4 mW·cm^{-2} at 405 nm), Ivocerin-containing resins – P0T3IVO2 and P3T3IVO2 – exhibited faster and more complete conversion of thiol and alkene groups compared to their TPO-L equivalents, P0T3L2 and P3T3L2. This can be explained by the higher quantum efficiency of Ivocerin compared to TPO-L ($\phi = 0.83$ [34] vs. $\phi = 0.30$ [35, 36]), allowing more efficient radical generation under the same light exposure. This effect is especially relevant in systems where radical inhibition by TMG is present, as the higher efficiency of Ivocerin can help partially overcome this kinetic limitation.

Third, the addition of PAG-Vi to the TMG-containing formulation led to surprising acceleration in cure kinetics regardless of the chosen photoinitiator component. Although PAG-Vi is designed to be inactive under visible light, its mere presence appears to reduce the effective basicity of TMG, possibly through acid-base interactions or complex formation. This attenuation of TMG's basicity diminishes the inhibitory effect of thiolate formation, allowing the radical propagation to proceed more efficiently. As a result, an unexpected increase in cure rate is observed even in the absence of PAG-Vi activation, suggesting a nuanced interplay between the basic catalyst and the acid generator.

In the end, it is important to compare the cure degree since it could significantly affect the material's relaxation properties in the UV-deactivated state. Therefore, a comprehensive evaluation of both kinetic profiles and final cure degree is necessary to optimize the orthogonal photochemical sequence for both performance and responsiveness.

To get a deeper insight into the possible mechanism, TMG and PAG-Vi were dissolved in DMSO-d_6 at equimolar concentrations and characterized using NMR spectroscopy (Figure 3). Monitoring the change in the ^{1}H-NMR spectra over a two-week period showed the appearance of new peaks and chemical shifts. The spectra revealed that progressive chemical shift changes and the appearance of new peaks, indicating ongoing chemical interaction between the two species in the absence of light. Notably, the vinyl protons of PAG-Vi (originally appearing as two well-defined doublets at δ = 6.03 and 5.52 ppm) exhibited gradual splitting and downfield shifts. The observed effect could be assigned to the interaction between the sulfone moiety and the base, suggesting that the interaction between PAG-Vi and TMG is not merely a static association but a dynamic process that evolves over time.

15213927, 2025, 22, Downloaded from https://onlinelibrary.wiley.com/doi/10.1002/marc.202500654 by Politecnico Di Torino Sist. Bibl Del Polit Di Torino, Wiley Online Library on [10/12/2025]. See the Terms and Conditions (https://onlinelibrary.wiley.com/terms-and-conditions) on Wiley Online Library for rules of use; OA articles are governed by the applicable Creative Commons License

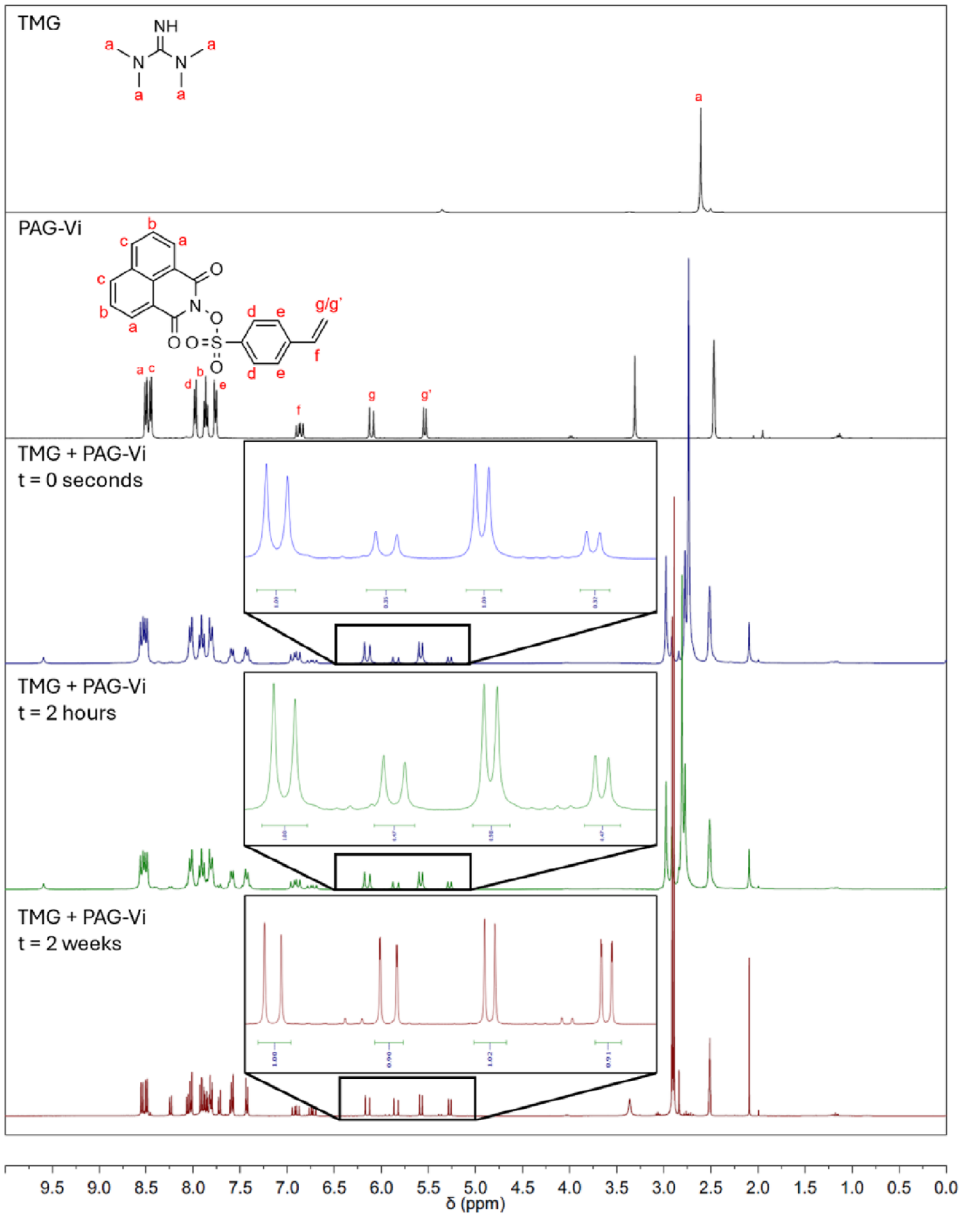

FIGURE 3 | ^{1}H NMR spectra of TMG, PAG-Vi, and equimolar TMG and PAG-Vi systems through time (300 MHz, DMSO-d_6).

In addition to the vinyl region, other proton environments showed significant changes. Broadening, peak splitting, and deshielding were observed for the methyl protons of TMG ($\delta \approx 2.68$ to 3.12 ppm), indicating a change in the electronic environments likely due to interactions with the sulfonate or aromatic groups of PAG-Vi whose peaks exhibited more complex spin–spin splitting patterns. Importantly, no signals appeared in the strong downfield region between 8 and 9 ppm, where imine protons would typically resonate. This absence confirms that no imine formation occurs and that PAG-Vi remains chemically intact and capable of photoactivation.

To further probe the nature of these interactions, a separate COSY experiment revealed no through-bond interaction between TMG and PAG-Vi ruling out covalent bond formation between the two species. Complementary ^{13}C-NMR spectroscopy further showed the appearance of at least twice the amount of peaks after reaching an equilibrium (Figure S3). These observations support the hypothesis that the interaction involves reversible acid-base interactions or the formation of ion pairs and transient adducts. Over time, the emergence of stabilized species hints at dynamic equilibrium processes wherein TMG may be partially protonated, thereby diminishing its catalytic basicity. The gradual shift and emergence of new signals indicate the formation of intermediate species or transient complexes that stabilize after an extended period. Such behavior implies that the basicity of TMG and the acidity of the PAG-Vi molecule may contribute to a reversible equilibrium, affecting the chemical environment of the system.

Complementing the NMR data, pH measurements were conducted in ethanol to monitor the evolution of acidity in various 1 mM mixtures (Table 2). TMG solutions alone exhibited a basic pH of 12.67, consistent with its strong nucleophilic character. Meanwhile, a 1:1 molar ratio between PAG-Vi and TMG decreased

15213927, 2025, 22, Downloaded from https://onlinelibrary.wiley.com/doi/10.1002/marc.202500654 by Politecnico Di Torino Sist. Bibl Del Polit Di Torino, Wiley Online Library on [10/12/2025]. See the Terms and Conditions (https://onlinelibrary.wiley.com/terms-and-conditions) on Wiley Online Library for rules of use; OA articles are governed by the applicable Creative Commons License

TABLE 2 | Recorded pH values of 1 mM stock solutions in ethanol.

Solution	pH initial	pH after exposure to 405 nm/ 450 nm	pH after exposure to 365 nm
TMG	12.67	—	—
PAG-Vi	7.57	6.32	2.20
TPO-L	7.03	2.84	—
Ivocerin	6.63	3.23	—
TMG, PAG-Vi	10.35	9.84	4.36
TMG, TPO-L	12.27	8.21	—
TMG, Ivocerin	12.59	8.57	—
TPO-L PAG-Vi	7.21	1.69	1.35
Ivocerin, PAG-Vi	7.32	1.69	1.32
TMG, PAG-Vi, TPO-L	9.32	4.44	3.85
TMG, PAG-Vi, Ivocerin	10.39	6.41	5.35

the starting pH to 10.35, reflecting partial neutralization and/or formation of an acid-base complex. The addition of TPO-L to the mixture (TMG:PAG-Vi:TPO-L = 1:1:1) further reduced the initial pH to 9.32. After sequential photoirradiation at 405 nm for 10 min and 365 nm for 45 min (47 J·cm^{-2} and 580 kJ·cm^{-2}, respectively), the final pH dropped markedly to 3.85. This stepwise acidification underscores the additive effect of each component on the system's net proton balance. Analogous measurements were performed in systems where TPO-L was replaced by Ivocerin. Results revealed a similar trend in decreasing pH values but with slightly less pronounced final acidification, suggesting differences in the acidic byproducts generated by the two photoinitiators.

What these findings propose is a more complex role played by the photoinitiator beyond radical generation. In particular, TPO-L is known to produce acidic phosphonyl radicals and phosphorus-containing degradation products upon irradiation, which can significantly reduce the pH of the medium [37, 38]. Mixing TPO-L and TMG did not result to a pH change until light exposure led to a measurable decrease in basicity. This inadvertent generation of acidic species likely also contributes to the partial neutralization of TMG, thereby reducing its catalytic activity. These have implications on the optimization of the stress relaxation kinetics of cured samples discussed in the next section.

2.2 | Wavelength-Dependent Stress Relaxation Kinetics

The objective of a photoswitchable CAN is to reach a drastic change in bond exchange kinetics and, consequently, stress relaxation behavior after light exposure. An ideal dynamic photopolymer shows a fast relaxation in VIS-cured state and a slow to non-response in the UV-deactivated state (neutralization of TMG due to the UV-released acidic species). To find the optimal resin composition of the photoswitchable polymer, VIS-cured and UV-deactivated samples were prepared and analyzed. All the VIS-cured samples were obtained by curing with either 405 or 450 nm light irradiation (79.3 mW·cm^{-2}) for 1 min each side, while UV-deactivated samples were obtained through subsequent irradiation of cured samples with 365 nm light (215.1 mW·cm^{-2}) for 15 min. Independent on the composition, the obtained photopolymers had a comparable crosslink degree as evidenced by DSC (T_g ranged between −32°C and −31°C) and swelling measurements (Figure S4 and Table S1, respectively). This is crucial as the network mobility affects stress relaxation kinetics. This structural uniformity ensures that differences in stress relaxation behavior can be attributed primarily to chemical factors rather than changes in network architecture.

While FTIR kinetics showed that formulations containing Ivocerin cured faster than those with TPO-L attributed to Ivocerin's higher quantum efficiency, this benefit did not translate to improved dynamic performance. As seen in Figure 4a, the Ivocerin-based system (P3T3IVO2) exhibited significantly slower relaxation than any TPO-L-based formulation. A slower relaxation profile could also be observed in Figure 4b with increasing photoinitiator concentration. Interestingly, the same behavior was observed even in the absence of PAG-Vi (Figure S5). These observations, as alluded by the pH test results, suggest that the photoinitiator or its photodegradation products may interfere with TMG's catalytic activity due to several possible phenomena: direct interaction between photoinitiator and base; interaction of the photodecomposition products with base or PAG-Vi; energy transfer of the excited state of the photoinitiator to the PAG-Vi, leading to its preliminary activation during the photocuring step. To eliminate the effect of energy transfer, another set of samples initially subjected to lower irradiation dose but with subsequent thermal postcuring for 1 h at 100°C were also measured. This approach yielded stress relaxation behavior similar to that of the fully photocured system, suggesting that a more complex, persistent interaction occurs in the polymer network, beyond simple photoactivation events. Based on these results, a photoinitiator concentration of 2 mol% TPO-L was selected as optimal for further studies. At this level, a balance was achieved between sufficient curing speed and acceptable dynamic response in the active state. The 3 mol% nominal value of TMG for these samples was chosen based on the recommended protocol of Bowman's group [23]. Earlier trials using lower concentrations of equimolar TMG and PAG-Vi (both at 1.5 mol%)

15213927, 2025, 22, Downloaded from https://onlinelibrary.wiley.com/doi/10.1002/marc.202500654 by Politecnico Di Torino Sist. Bibl Del Polit Di Torino, Wiley Online Library on [10/12/2025]. See the Terms and Conditions (https://onlinelibrary.wiley.com/terms-and-conditions) on Wiley Online Library for rules of use; OA articles are governed by the applicable Creative Commons License

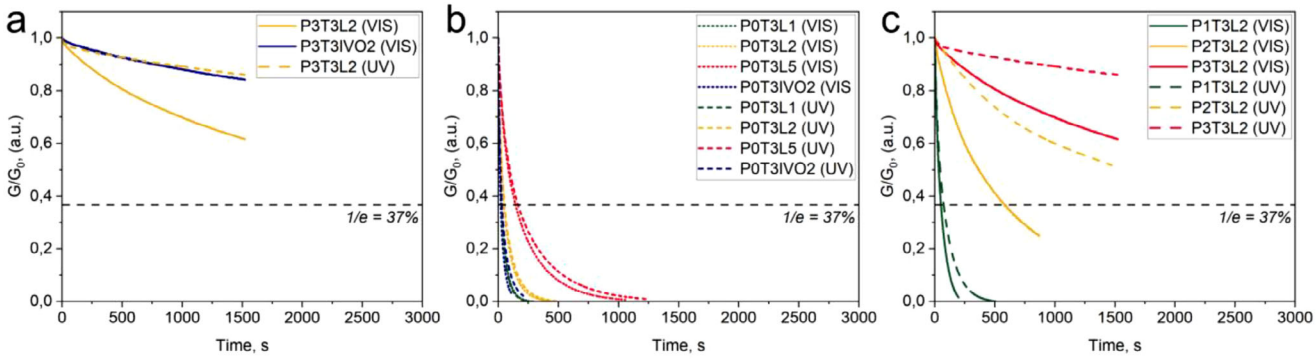

FIGURE 4 | Superimposed stress relaxation curves grouped based on the varying (a) photoinitiator, (b) photoinitiator concentration, and (c) PAG-Vi concentration. Stress relaxation measurements were done at a constant temperature of 60°C.

produced samples not prone to stress relaxation (Figure S6). This additionally indicates a more prominent partial neutralization or complexation of the base when less than 3 mol% is present.

With the TPO-L and TMG concentrations fixed, the influence of PAG-Vi concentration (1–3 mol%) on stress relaxation was investigated next. Figure 4c shows an increasing relaxation time as more PAG-Vi was introduced to the resin formulation. Increasing the PAG-Vi concentration affected the behavior in two aspects.

First, the time it took to reach a 1/e or $G_T/G_0 = 0.37$ (τ^*) of photopolymers in the VIS-cured state increased with rising PAG-Vi concentration. This means that the catalytic efficiency of TMG had been compromised by the presence of PAG-Vi even before the acid got released to the system. This is in good agreement with the previously observed shift in the pH value of TMG after incorporation of PAG-Vi.

Second, after UV-deactivation, the difference in relaxation time (τ^*) between the cured and deactivated states became more pronounced with increasing PAG-Vi content. At 1 mol% of PAG-Vi (P1T3L2), the stress relaxation time was very close to the PAG-free reference system (i.e., 50 s for 1 mol% PAG-Vi and 46 s for PAG-Vi-free system). Although the catalytic efficiency of 3 mol% TMG was not significantly affected by the lower PAG-Vi content, almost no deactivation effect was seen for the UV-deactivated state of P1T3L2. This indicates that the amount of photoacid generated post-UV exposure was insufficient for full deactivation, and TMG remained largely active. Increasing the PAG-Vi content to 2 mol% (P2T3L2) led to a significant slowing down of the stress relaxation of the VIS-cured sample ($\tau^* = 576$ s) due to the interaction between PAG-Vi and TMG. However, deactivation didn't lead to a complete stop of the exchange reactions, resulting in gradual stress relaxation ($\tau^* = 2500$ s) in the UV-deactivated P2T3L2. When equimolar amounts (3 mol%) of PAG-Vi and TMG were present in the system, VIS-cured P3T3L2 showed slow stress relaxation ($\tau^* = 3100$ s), but the UV-deactivated counterpart showed practically no stress relaxation within the observed timeframe. These results indicate that a 1:1 molar ratio between TMG and PAG-Vi is necessary and sufficient for complete deactivation under UV exposure.

Since the addition of the PAG-Vi strongly affects the stress relaxation behavior of the cured sample, the search for a more suitable base catalyst was undertaken. Choosing the appropriate transthioesterification catalyst has been comprehensively investigated by Bowman's group [23, 37]. Generally, organic bases with high basicity and/or nucleophilicity were reported to catalyze this type of exchange reaction most efficiently. Figure S7 shows the effect of the variation on the basic catalyst included in the resin formulation. Two tertiary amines with high nucleophilicity, 1,4-diazabicyclo[2.2.2]octane (DABCO) and 1,5-diazabicyclo[4.3.0]non-5-ene (DBN) had been evaluated whether they could deliver better performance than TMG. It can be inferred from the curves that all these catalysts provide fast stress relaxation with all of them relaxing within 60 s. However, the addition of PAG-Vi slowed down the stress relaxation of DABCO- and DBN-containing formulations even to a higher degree than those with TMG. Thus, further experiments were carried out with P3T3L2, whose bond exchange kinetics could be switched off in the UV-deactivated state whilst still having rapid stress relaxation in the original VIS-cured state.

2.3 | Local Deactivation of Bond Exchange Reactions

To demonstrate the spatial control on the topological rearrangement of the optimized thiol-thioester photopolymer, imprinting and reshaping experiments were performed on the optimized polymer formulation, containing 2 mol.% of TPO-L, 3 mol.% of TMG, 3 mol.% of PAG-Vi.

In the first step, pristine images after subjecting a treated square disc to confocal microscopy can be seen in Figure 5a–c. The UV-deactivated top side did not replicate as much of the stamp compared to the VIS-cured bottom side, which evidences that topological rearrangements are faster for the side not exposed to 365 nm. The deactivated side managing to take a faded imprint can be explained by the non-zero stress relaxation of UV-deactivated P3T3L2 (see also stress relaxation data in Figure 4). The VIS-cured and UV-deactivated imprints have mean z-heights of 54 μm and less than 1 μm, respectively.

In another demonstration, the single-time shape memory ability of the P3T3L2 formulation was tested. A tell-tale change in color

15213927, 2025, 22, Downloaded from https://onlinelibrary.wiley.com/doi/10.1002/marc.202500654 by Politecnico Di Torino Sist. Bibl Del Polit Di Torino, Wiley Online Library on [10/12/2025]. See the Terms and Conditions (https://onlinelibrary.wiley.com/terms-and-conditions) on Wiley Online Library for rules of use; OA articles are governed by the applicable Creative Commons License

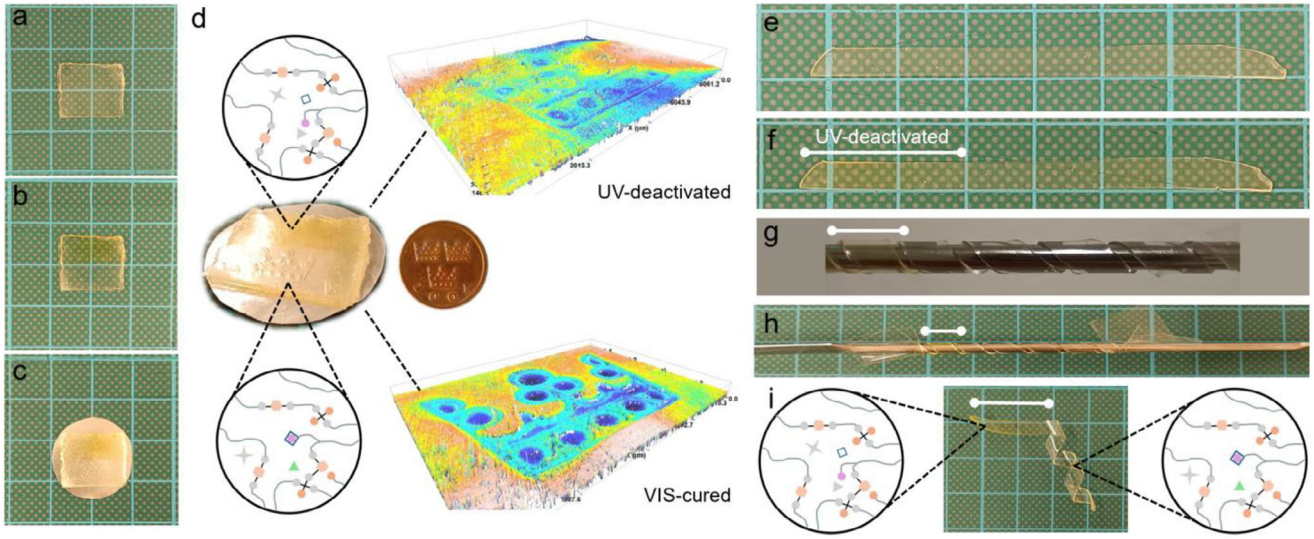

FIGURE 5 | Coin imprinting of (a) VIS-cured square disc, (b) UV-deactivation of the top part, (c) disc after stamping, and (d) insets of the 3D reconstructed images. Reshaping of (e) VIS-cured strip, (f) UV-deactivation of the left side, (g) twisting of the strip to the rod, (h) twisted strip secured on both ends, and (i) shape memory ability of the UV-deactivated side.

from clear to yellow can be observed after the UV-deactivation of the exposed side. The strip was then twisted to a stainless-steel bar with a diameter of 6 mm and secured at both ends with clear sticky tape. This was placed in the oven at T = 80°C for 30 min before unwrapping the strip. Figure 5e–i shows the UV-deactivated side returning to its original flat conformation while the VIS-cured side reconfigured to a helical shape after cooling the set-up to room temperature and unwrapping the strip from the metal rod. This clearly demonstrates the spatially resolved bond exchange between the thiol and thioester moieties of the optimized covalent adaptable network.

3 | Conclusion

This study presents a comprehensive approach to designing and optimizing locally deactivatable thiol-thioester vitrimers. It was shown that a thiol-ene network having a covalently attachable PAG (PAG-Vi) could be cured under visible light irradiation and subsequently be deactivated by the photolysis of PAG-Vi after UV irradiation under 365 nm light irradiation, the process was shown to be spatially controllable, allowing surface patterning and reshaping at moderately high temperatures. However, for the studied system, the stress relaxation behavior and photoswitchability of the network is also highly dependent on intricate interactions between resin components.

Stress relaxation kinetics of the VIS-cured samples (exposed only to visible light for curing) showed the sensitivity to both photoinitiator type and its concentration. Specifically, TPO-L was identified as a more suitable photoinitiator than Ivocerin due to its lower interference with network dynamics. Increasing concentrations of TPO-L were shown to impede stress relaxation even prior to UV exposure, highlighting non-negligible base deactivation and molecular interactions in the formulation. In addition, this effect was evidenced by the drop of the pH of solutions containing TPO-L and TMG after the visible light irradiation.

Furthermore, the stress relaxation kinetics were more affected by the strong interaction between TMG and PAG-Vi. The addition of PAG-Vi in the system led to a significant increase to the stress relaxation time for visible light treated samples (from 47 s for PAG-free system to 2500 s for 3 mol% of PAG-Vi). NMR studies of equimolar mixtures of TMG and PAG-Vi elucidated the effect, thereby showing the shift in the signals of the components and evidencing non-covalent interactions between the two compounds. The methyl group peaks of TMG were found to shift downfield, evidencing the lower electron density and hence lower nucleophilicity of the base. In addition, the pH studies showed a crucial decrease in the basicity of the TMG-PAG-Vi mixture in comparison with the pure TMG prior to any irradiation. Hence, a 1:1 molar ratio between PAG-Vi and TMG (3 mol%) was found to be the most optimal, maintaining a balance of fast stress relaxation in the VIS-cured state and slower kinetics in the UV-deactivated state. Our findings also underscore the necessity of controlling crosslink density, exposure conditions, and aging effects to ensure reproducible and tunable material properties stemming from chemical factors' bond exchange modulation rather than changes in network architecture.

The optimized system was used for the demonstration of the ability to spatially control network deactivation. The cured sample was imprintable at 80°C within 30 min, resulting in the average depth of the pattern of 54 μm, while the UV-exposed sample demonstrated almost no imprintability, with the average depth of the pattern to be <1 μm. Locally controlled patterning and reshaping allow the application of this concept for reconfigurable surfaces, adaptive materials, and shape memory polymers. While challenges persist regarding side reaction mitigation and catalyst optimization, this work provides a foundational methodology for developing photoswitchable vitrimers with tunable properties. The procedural approach presented herein offers both novice and experienced researchers a practical roadmap for further advancing thiol-thioester dynamic bond exchange systems toward increasingly sophisticated applications such as reconfigurable microdevices and smart coatings.

15213927, 2025, 22, Downloaded from https://onlinelibrary.wiley.com/doi/10.1002/marc.202500654 by Politecnico Di Torino Sist. Bibl Del Polit Di Torino, Wiley Online Library on [10/12/2025]. See the Terms and Conditions (https://onlinelibrary.wiley.com/terms-and-conditions) on Wiley Online Library for rules of use; OA articles are governed by the applicable Creative Commons License

Acknowledgements

R.K. and J.V.T. contributed equally to this work. This project has received funding from the EU's Horizon 2021 programme under the Marie Skłodowska-Curie Doctoral Networks (MSCA-DN) grant agreement No 101073432. Part of the research work was also carried out within the COMET-Module project "Repairtecture" (project-no.: 904927) at the Polymer Competence Center Leoben GmbH (PCCL, Austria) within the framework of the COMET-program of the Federal Ministry for Climate Action, Environment, Energy, Mobility, Innovation and Technology and the Federal Ministry of Labour and Economy. Funding was received by the Austrian Government and the State Governments of Styria and Upper Austria.

Open Access funding provided by Montanuniversitat Leoben/KEMÖ.

Conflicts of Interest

The authors declare no conflicts of interest.

Data Availability Statement

The data that support the findings of this study are available from the corresponding author upon reasonable request.

References

1. M. Capelot, M. M. Unterlass, F. Tournilhac, and L. Leibler, "Catalytic Control of the Vitrimer Glass Transition," *ACS Macro Letters* 1, no. 7 (2012): 789–792.

2. F. Garcia and M. M. J. Smulders, "Dynamic Covalent Polymers," *Journal of Polymer Science Part A: Polymer Chemistry* 54 (2016): 3551–3577.

3. M. Capelot, D. Montarnal, F. Tournilhac, and L. Leibler, "Metal-Catalyzed Transesterification for Healing and Assembling of Thermosets," *Journal of the American Chemical Society* 134, no. 18 (2012): 7664–7667.

4. A. Breuillac, A. Kassalias, and R. Nicolaÿ, "Polybutadiene Vitrimers Based on Dioxaborolane Chemistry and Dual Networks With Static and Dynamic Cross-Links," *Macromolecules* 52, no. 18 (2019): 7102–7113.

5. O. Konuray, X. Fernández-Francos, and X. Ramis, "Structural Design of CANs With Fine-Tunable Relaxation Properties: A Theoretical Framework Based on Network Structure and Kinetics Modeling," *Macromolecules* 56, no. 13 (2023): 4855–4873.

6. V. Zhang, B. Kang, J. V. Accardo, and J. A. Kalow, "Structure–Reactivity–Property Relationships in Covalent Adaptable Networks," *Journal of the American Chemical Society* 144, no. 49 (2022): 22358–22377.

7. P. Chakma and D. Konkolewicz, "Dynamic Covalent Bonds in Polymeric Materials," *Angewandte Chemie International Edition* 58, no. 29 (2019): 9682–9695.

8. W. Zou, J. Dong, Y. Luo, Q. Zhao, and T. Xie, "Dynamic Covalent Polymer Networks: From Old Chemistry to Modern Day Innovations," *Advanced Materials* 29, no. 14 (2017): 1606100.

9. D. J. Fortman, J. P. Brutman, and G. X. De Hoe, "Approaches to Sustainable and Continually Recyclable Cross-Linked Polymers," *ACS Sustainable Chemistry & Engineering* 6, no. 9 (2018): 11145–11159.

10. M. Guerre, C. Taplan, J. M. Winne, and F. E. D. Prez, "Vitrimers: Directing Chemical Reactivity to Control Material Properties," *Chemical Science* 11, no. 19 (2020): 4855–4870.

11. W. Denissen, J. M. Winne, and F. E. D. Prez, "Vitrimers: Permanent Organic Networks With Glass-Like Fluidity," *Chemical Science* 7, no. 1 (2015): 30–38.

12. W. Alabiso and S. Schlögl, "The Impact of Vitrimers on the Industry of the Future: Chemistry, Properties and Sustainable Forward-Looking Applications," *Polymers* 12, no. 8 (2020): 1160.

13. Y. Yang, Y. Xu, Y. Ji, and Y. Wei, "Functional Epoxy Vitrimers and Composites," *Progress in Materials Science* 120 (2021): 100710.

14. R. Avshalomov, N. Jarach, and H. Dodiuk, "Breaking the Unbreakable Bond: Towards Sustainable Adhesives' Future," *European Polymer Journal* 209 (2024): 112920.

15. M. Guerre, C. Taplan, J. M. Winne, and F. E. Du Prez, "Vitrimers: Directing Chemical Reactivity to Control Material Properties," *Chemical Science* 11, no. 19 (2020): 4855–4870.

16. J. Zheng, Z. M. Png, and S. H. Ng, "Vitrimers: Current Research Trends and Their Emerging Applications," *Materials Today* 51 (2021): 586–625.

17. N. J. Van Zee and R. Nicolaÿ, "Vitrimers: Permanently Crosslinked Polymers With Dynamic Network Topology," *Progress in Polymer Science* 104 (2020): 101233.

18. D. Montarnal, M. Capelot, F. Tournilhac, and L. Leibler, "Silica-Like Malleable Materials From Permanent Organic Networks," *Science* 334, no. 6058 (2011): 965–968.

19. K. Li, N. V. Tran, and Y. Pan, "Next-Generation Vitrimers Design Through Theoretical Understanding and Computational Simulations," *Advanced Science* 11, no. 5 (2024): 2302816.

20. B. T. Worrell, S. Mavila, and C. Wang, "A User's Guide to the Thiol-Thioester Exchange in Organic Media: Scope, Limitations, and Applications in Material Science," *Polymer Chemistry* 9, no. 36 (2018): 4523–4534.

21. D. Reisinger, A. Sietmann, and A. Das, "Light-Driven, Reversible Spatiotemporal Control of Dynamic Covalent Polymers," *Advanced Materials* 36, no. 47 (2024): 2411307, https://doi.org/10.1002/adma.202411307.

22. B. T. Worrell, M. K. McBride, and G. B. Lyon, "Bistable and Photoswitchable States of Matter," *Nature Communications* 9 (2018): 2804.

23. J. J. Hernandez, S. P. Keyser, A. L. Dobson, A. S. Kuenstler, and C. N. Bowman, "Modeling Degradation of Thioester Networks Controlled by Oligomer Structures and Thiol–Thioester Exchange," *Macromolecules* 57, no. 4 (2024): 1426–1437.

24. C. Wang, S. Mavila, B. T. Worrell, W. Xi, T. M. Goldman, and C. N. Bowman, "Productive Exchange of Thiols and Thioesters to Form Dynamic Polythioester-Based Polymers," *ACS Macro Letters* 7, no. 11 (2018): 1312–1316.

25. E. Rossegger, K. Moazzen, M. Fleisch, and S. Schlögl, "Locally Controlling Dynamic Exchange Reactions in 3D Printed Thiol-Acrylate Vitrimers Using Dual-Wavelength Digital Light Processing," *Polymer Chemistry* 12, no. 21 (2021): 3077–3083.

26. R. Korotkov, W. Alabiso, and A. Jelinek, "Microscale Manipulation of Bond Exchange Reactions in Photocurable Vitrimers With a Covalently Attachable Photoacid Generator," *Chemical Science* 15, no. 39 (2024): 16271–16280.

27. Y. Yang, Z. Pei, X. Zhang, L. Tao, Y. Wei, and Y. Ji, "Carbon Nanotube–Vitrimer Composite for Facile and Efficient Photo-Welding of Epoxy," *Chemical Science* 5, no. 9 (2014): 3486–3492.

28. Z. Wang, Z. Li, Y. Wei, and Y. Ji, "Gold Nanospheres Dispersed Light Responsive Epoxy Vitrimers," *Polymers* 10, no. 1 (2018): 65, https://doi.org/10.3390/polym10010065.

29. W. Alabiso, B. Sölle, and D. Reisinger, "On-Demand Activation of Transesterification by Chemical Amplification in Dynamic Thiol-Ene Photopolymers," *Angewandte Chemie International Edition* 62 (2023): 202311341.

30. W. Alabiso, Y. Li, J. Brancart, G. V. Assche, E. Rossegger, and S. Schlögl, "The Use of a Sulfonium-Based Photoacid Generator in Thiol–Ene Photopolymers for the Controlled Activation of Transesterification Through Chemical Amplification," *Polymer Chemistry* 15, no. 4 (2024): 321–331.

31. E. Rossegger, U. Shaukat, K. Moazzen, M. Fleisch, M. Berer, and S. Schlögl, "The Effect of Photolatent Catalysts on the Exchange

15213927, 2025, 22, Downloaded from https://onlinelibrary.wiley.com/doi/10.1002/marc.202500654 by Politecnico Di Torino Sist. Bibl Del Polit Di Torino, Wiley Online Library on [10/12/2025]. See the Terms and Conditions (https://onlinelibrary.wiley.com/terms-and-conditions) on Wiley Online Library for rules of use; OA articles are governed by the applicable Creative Commons License

Kinetics of Dual-Wavelength 3D Printable and Photopatternable Thiol-Click Vitrimers," *Polymer Chemistry* 14, no. 21 (2023): 2640–2651.

32. D. Reisinger, S. Kaiser, E. Rossegger, W. Alabiso, B. Rieger, and S. Schlögl, "Introduction of Photolatent Bases for Locally Controlling Dynamic Exchange Reactions in Thermo-Activated Vitrimers," *Angewandte Chemie International Edition* 60, no. 26 (2021): 14302–14306.

33. D. M. Love, B. D. Fairbanks, and C. N. Bowman, "Evaluation of Aromatic Thiols as Photoinitiators," *Macromolecules* 53, no. 13 (2020): 5237–5247.

34. A. Eibel, D. E. Fast, and G. Gescheidt, "Choosing the Ideal Photoinitiator for Free Radical Photopolymerizations: Predictions Based on Simulations Using Established Data," *Polymer Chemistry* 9, no. 41 (2018): 5107–5115.

35. K. Dietliker, A compilation of photoinitiators commercially available for UV today, SITA Technology Limited, 180, 2001.

36. S. Jockusch, I. V. Koptyug, P. F. McGarry, G. W. Sluggett, N. J. Turro, and D. M. Watkins, "A Steady-State and Picosecond Pump-Probe Investigation of the Photophysics of an Acyl and a Bis(acyl)phosphine Oxide," *Journal of the American Chemical Society* 119, no. 47 (1997): 11495–11501.

37. J. A. Rossi-Ashton, A. K. Clarke, W. P. Unsworth, and R. J. K. Taylor, "Phosphoranyl Radical Fragmentation Reactions Driven by Photoredox Catalysis," *ACS Catalysis* 10, no. 13 (2020): 7250–7261.

38. Y. Wu, S. Joseph, and N. R. Aluru, "Effect of Cross-Linking on the Diffusion of Water, Ions, and Small Molecules in Hydrogels," *The Journal of Physical Chemistry B* 113, no. 11 (2009): 3512–3520.

Supporting Information

Additional supporting information can be found online in the Supporting Information section.

Supporting File: marc70065-sup-0001-SuppMat.docx.

15213927, 2025, 22, Downloaded from https://onlinelibrary.wiley.com/doi/10.1002/marc.202500654 by Politecnico Di Torino Sist. Bibl Del Polit Di Torino, Wiley Online Library on [10/12/2025]. See the Terms and Conditions (https://onlinelibrary.wiley.com/terms-and-conditions) on Wiley Online Library for rules of use; OA articles are governed by the applicable Creative Commons License